JOURNAL OF MATERIALS SCIENCE 27 (1992) 6411–6416

Failure mechanisms in impacting penetrators

R. L. WOODWARD, R. G. O'DONNELL, C. J. FLOCKHART
DSTO Materials Research Laboratory, PO Box 50, Ascot Vale, 3032 Victoria, Australia

Experiments are described on (i) the simple Taylor test where a flat-ended projectile mushrooms against a semi-infinite "rigid target", (ii) penetration of conically tipped cylindrical projectiles into semi-infinite targets, (iii) the use of modified nose geometries to direct the pattern of shear failure and (iv) the impact of balls on thin plates. Macro- and micro-structural investigation of fractured penetrators illustrates mechanisms of ductile fracture, intergranular and transgranular brittle fractures, and adiabatic shear. Stress analysis highlights those regions subjected to prolonged hydrostatic tensile stresses during impact indicating fracture by spalling, and those regions where persistent velocity discontinuities or planes of maximum shear strain rate indicate adiabatic shear failure.

1. Introduction

Normal impact of a projectile at sufficiently high velocity results in plastic deformation and possibly failure, even against soft targets, because the change in momentum produces sufficiently high stress levels to exceed the yield or fracture stress of the projectile. The simplest configuration for the study of projectile deformation is the Taylor test [1] in which a flat-ended cylindrical projectile strikes a hard target, and the projectile deformation on the impact end is described as mushrooming. Analysis of the Taylor test assumes a rigid plastic solid. On impact with the hard target the yield stress is exceeded in the projectile cylinder, and the stationary mushroomed end is separated by a discontinuity from the undeformed section, which continues to move forward. Simplified and more exact graphical procedures were developed by Taylor [1] to relate final measured projectile deformed and undeformed lengths to the yield strength. Extensive experimental studies have shown that the one-dimensional Taylor analysis does not correctly predict projectile profiles, and derived yield strength values are, at best, approximate [2, 3]. Nevertheless, despite its quantitative shortcomings, the Taylor model is a useful description of the physics of impact. There have been a number of theoretical developments of the model [4–6], including the considerations of Jones and co-workers [7, 8] that the concept of a large step velocity change as material crosses the rigid–plastic boundary is unrealistic. Amongst others, Wilkins and Guinan [9] demonstrated far better simulations of projectile final profile using a two-dimensional axisymmetric finite difference approach. Papirno *et al.* [10] noted that strength data derived using simplified one-dimensional approaches to the Taylor test were a function of initial height to diameter ratio, and they also identified failure in the Taylor test in the form of the separation of a conical section from the impact end of the projectile, a phenomenon which has since been noted by others [11].

The separation of a conical region at the impact end in the Taylor test has its analogy in the separation of the projectile nose along a conical surface of intensive shear in projectile penetration studies [12–14], and is evident in flash radiographic images of break-up in high-speed fragment impacts [15]. Projectile penetration behaviour can be markedly affected by projectile geometry [16], and the shear failures described above have also been shown to be linked to ballistic performance [13, 17, 18].

The present work reviews some of the failure modes observed in impact by low length-to-diameter ratio (< 6) projectiles in relation to their material properties, microstructure, and an impact stress analysis. The method examines the conditions of strain, strain rate, stress deviator and hydrostatic stress as revealed by two-dimensional axisymmetric finite-element simulations using the DYNA 2D finite-element code [19]. The use of the Taylor test, conically tipped cylinder and ball impacts enables a variety of failure types to be observed.

2. Failure in the Taylor test

Fig. 1 shows steel Taylor test cylinders illustrating mushrooming of the impact end as well as shear and tensile fracturing. In the sample which has not fragmented, tensile splitting at the periphery of the mushroomed end is evident. (Fig. 1a.). In some cases a conical region separates by shear fracture, (Fig. 1b), and in other examples spiral shear fractures combine with the tensile cracking to separate the mushroomed material producing a conical profile at the impact end (Fig. 1c). Full representation of the tensile and spiral shear surfaces requires a three-dimensional simulation of the deformation. However, some failure surfaces can be described in terms of velocity discontinuities identified by regions of maximum shear strain rate. Thus the contours represented in the impact simulation of Fig. 2a and b at 10 and 8 μs after impact,

0022–2461

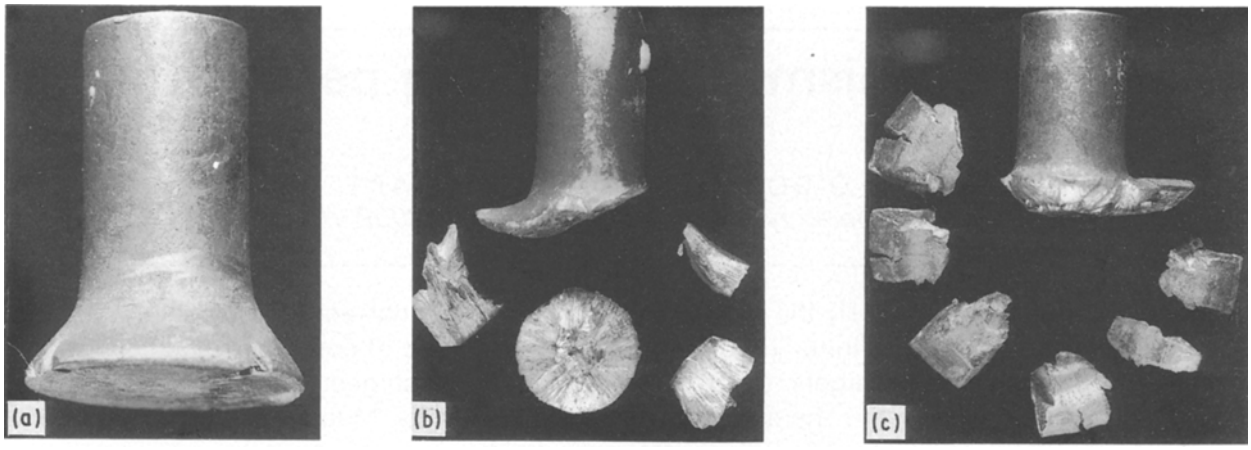

Figure 1 Typical steel Taylor test cylinders after impact showing (a) mushrooming of the impact end and splitting, due to the hoop strain exceeding material ductility, (b) formation and separation of a cone by shear, and (c) separation of mushroomed material by failure on spiral shear surfaces to produce a pointed profile.

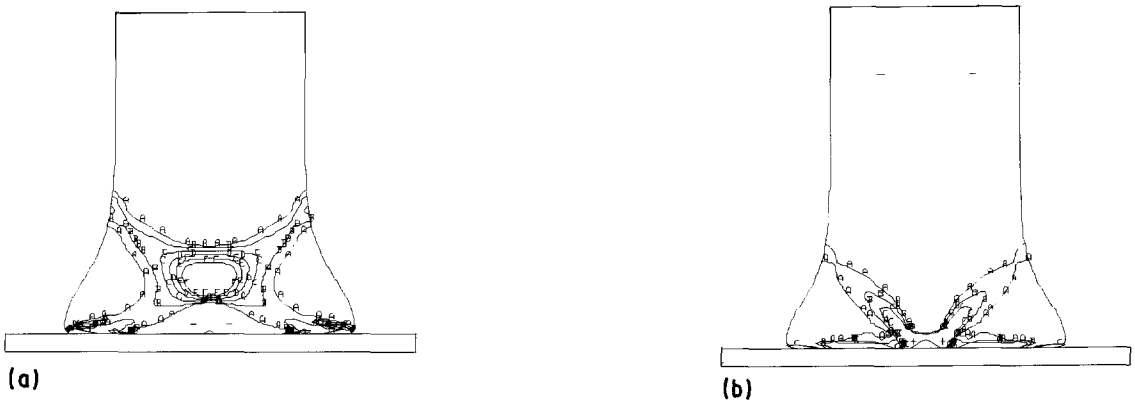

Figure 2 Shear strain-rate contours in the DYNA 2D simulation of mushrooming showing maxima in regions that correspond to (a) the formation and separation of a cone and (b) the production of a pointed profile at the nose of the projectile.

respectively, correlate with the shear failure surfaces in Fig. 1b and c, respectively. These failures occur by an adiabatic shear mechanism [20–28] whereby thermal softening requires that slip continue within a narrow band, a mechanism which is not predicted on the basis of effective strain [27]. The failure is achieved by deformation along a set of velocity discontinuities analogous to those derived from plane strain slip-line field solutions [20, 27]. The persistence of the alternative discontinuity patterns in Fig. 2 is governed by interfacial friction conditions as well as impact velocity and projectile strength, and this determines the nature of the failure. A further failure mode in the Taylor test, noted by Grady and Kipp [29], is void nucleation which correlates with a build-up of hydrostatic tension just behind the centre of impact in the Taylor test cylinder. This build-up of hydrostatic tension results from the interaction of stress relief waves from the cylinder sides, and the time at which the tensile stress is observed as well as its magnitude can be altered simply by changing the cylinder diameter.

3. Penetrator failure

Failures analogous to the separation of a cone within the impact end of a Taylor test projectile (Fig. 1b) have also been reported [13, 14] in perforation of targets by conical-tipped cylindrical projectiles, an example of which is illustrated in Fig. 3a. Notable is the small amount of deformation in the conical nose region and its separation from the rear of the penetrator by a zone of intense shear deformation. Such behaviour influences penetrator performance, particularly at low impact velocities [13, 17, 18]. The deformation behind the nose in Fig. 3a is typical of that described in modified Bernoulli [30, 31] or mushrooming/shear [32] models for high-velocity impact deformation of blunt penetrators. The deformation geometry of Fig. 3a can be reproduced by simulation (Fig. 3b), with deformation concentrated in areas of maximum shear strain rate or velocity discontinuity. Changing nose geometry can radically alter performance [17, 18] by changing the resistance of the penetrator to compression at low velocities, and the velocity at which nose separation occurs for conical penetrators [14]. Changes in nose geometry can be used to change the deformation mode, as in the case of Fig. 4 which shows a symmetrical peeling by shear when the conical nose of a projectile was truncated by a hollow cylindrical recess of depth approximately one half calibre. The shear failures being described are often of the adiabatic shear type; however, conventional shear fractures by mechanisms of nucleation, growth and linkage of voids or microcracks are not excluded, and are observed in less ductile penetrator materials.

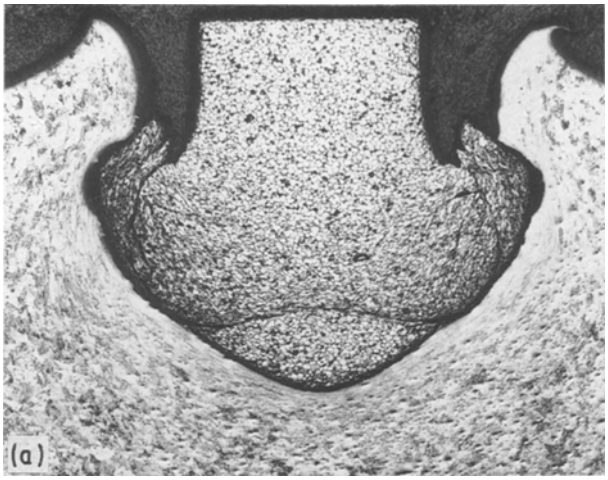

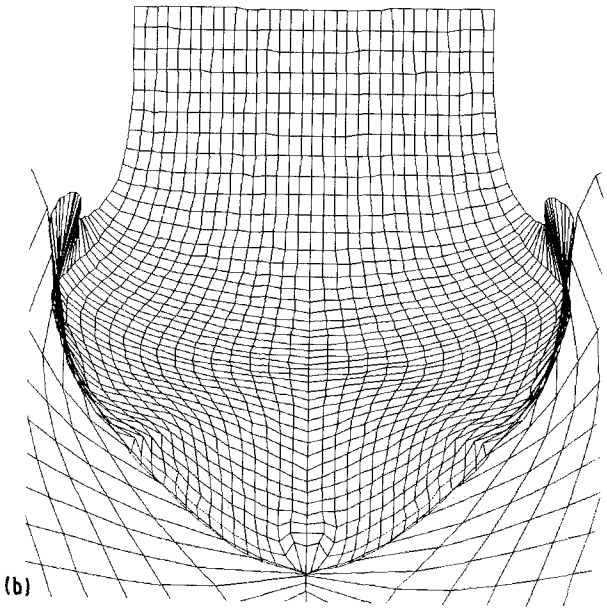

Figure 3 (a) Section through a tungsten alloy penetrator fired into a steel target and (b) DYNA-2D simulation showing the deformation by a geometry plot.

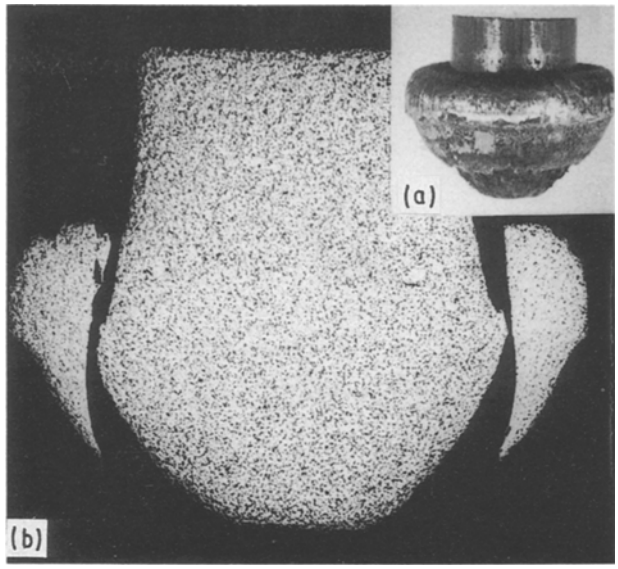

Figure 4 (a) Photograph and (b) section through a penetrator which has sheared to remove symmetrically the nose. The original shape of the projectile presented a 90° conical tip with a small cylindrical hole drilled vertically into the nose.

4. Impact failure of balls

Illustrated in Fig. 5 are a range of failures in high-strength steel balls with individual failure types labelled S for erosion by a shear mechanism, C for cone formation, E for exfoiliation, and T for tensile failures. The erosion, S, occurs by adiabatic shear, as identified by intense white etching bands along the edge of the failure zone. The uneroded portion closer to the centre of the impact area appears to be the result of a "dead zone" with no relative target/ball motion, a consequence of lower shear stress. The cone fracture, C, was also identified as occurring by adiabatic shear. It correlates with a simple velocity discontinuity bounded "dead zone" at the centre of impact (see below), and with a maximum in the shear strain rate as exhibited by similar features observed for Taylor test mushrooming and penetrator failure. In this case the DYNA 2D simulation also indicated a hydrostatic tension to occur in this region a few microseconds after impact. Some tensile cracks normal to the plane of impact are observed as a result of the compression of the cone. It has been found that a network of shear bands can occur within the ball (Fig. 6), which suggests that shear bands form, then cease to be active and are replaced by others, as the deformation geometry changes during impact.

The failures designated exfoiliation, E, in Fig. 5 appear to be strain-induced and are associated with metallurgical inhomogeneity in the balls. The exfoiliation cracks, as with all observed tension cracks, were predominantly intergranular to prior austenite grain boundaries, with a small amount of cleavage of the tempered martensite. Longitudinal cracking of the ball surface associated with a tensile hoop strain because of the ball compression has been linked by the intergranular fracture separating a thin layer at the surface in many cases. These intergranular fractures predominated in the region joining an outer harder layer to a softer core, the regions of different hardness also responding differently to etching.

In a significant number of tests the longitudinal cracks in the case continued through the balls splitting them into two hemispheres along the axis of impact. The DYNA 2D simulation indicates that the centre of the ball experiences both high hydrostatic and high radial tensions during impact. The fact that such splitting is only sometimes observed indicates that a favourable orientation of the metallurgical structure to impact as well as the correct impact velocity/target response is required. No indicative inclusion or defect orientation could be identified by optical microscopy of balls thus fractured. Also noted as fractures attributed to hydrostatic tension, T, are small fractures at the 10 and 2 o'clock positions (Fig. 5). These were also observed in tungsten alloy balls along with general opening of small individual cleavage and intergranular cracks through the half of the ball away from impact. This whole region is subject to hydrostatic tension at several stages during impact, and these hydrostatic tensions are also expected to assist with

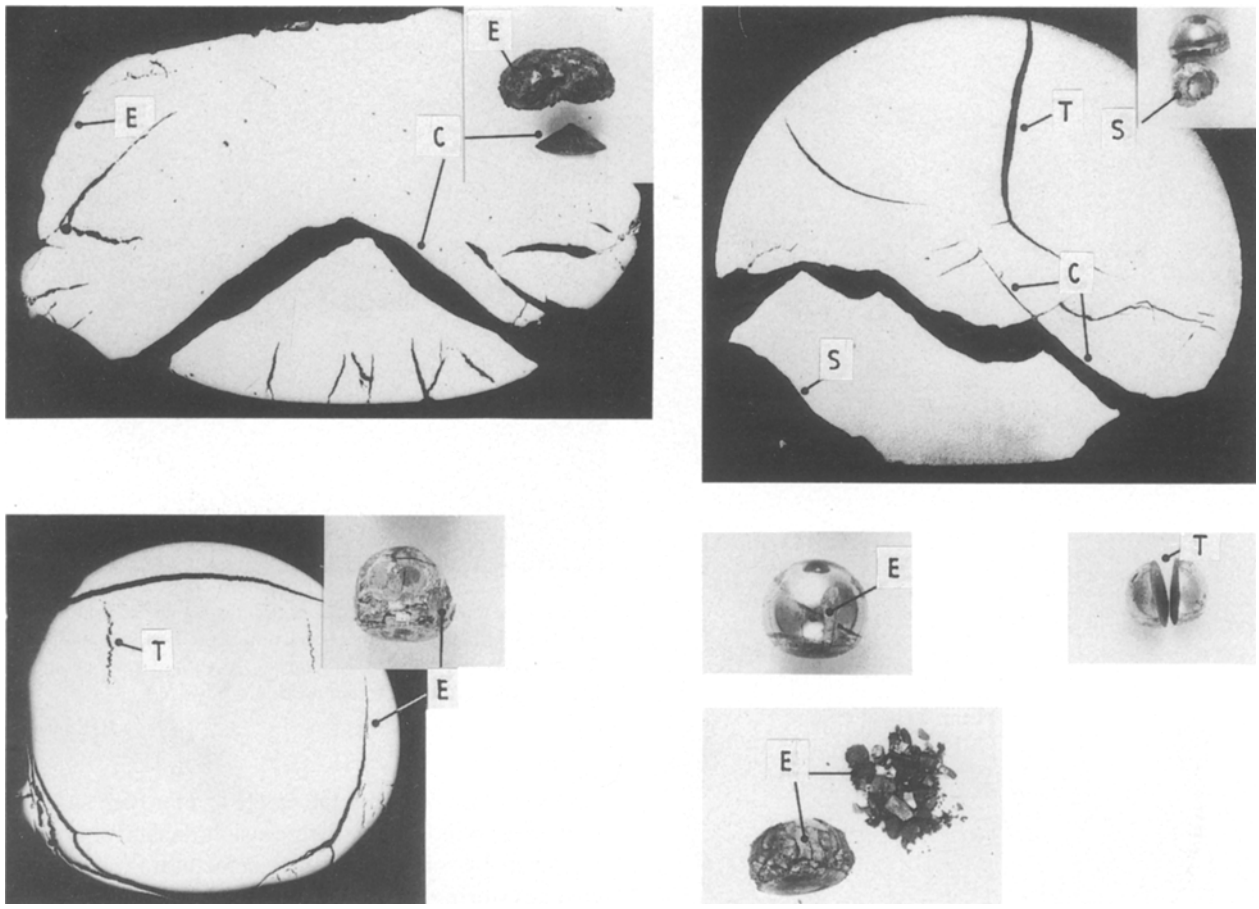

Figure 5 Typical failures and corresponding sections of impacted steel balls. The failures are identified by symbols discussed in the test.

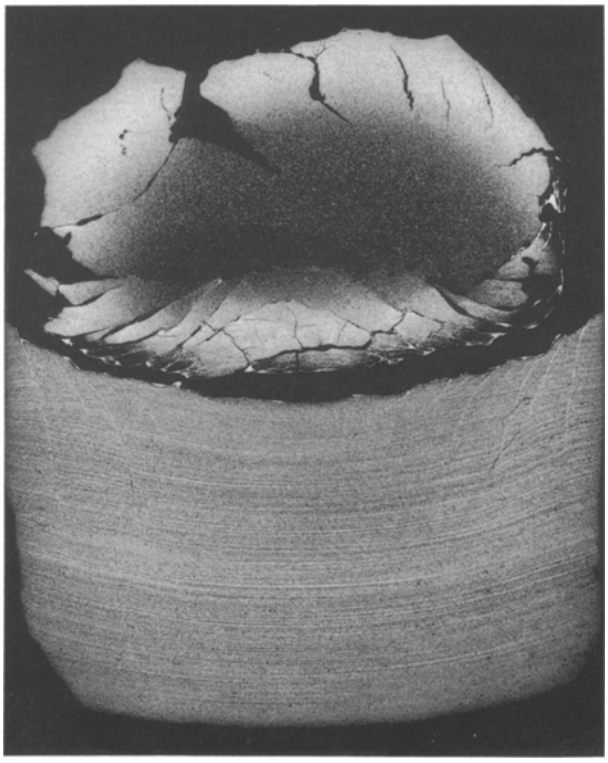

Figure 6 Steel ball and plug from perforation of a steel target plate showing the network of shear bands in the compressed ball and some surface fracture due to spalling.

the strain-induced exfoiliation cracking discussed above.

Some of the features noted in impact can be physically simulated in quasi-static compression of steel balls. Fig. 7a shows a section of a steel ball which has fractured into two hemispheres in simple compression: a conical region has separated on one compression face and the same feature is incipient at the other. A micrograph indicates a fine, white etching shear band in the latter case (Fig. 7b). The fracture through the centre is intergranular as in the impacts above and in many cases exfoiliation cracking was also observed. Fig. 7c shows the contours of maximum shear strain rate which would suggest again that the shear band occurs on a velocity discontinuity. The occurrence of "adiabatic" shear bands at low strain rate indicates an inherent instability of the steel, i.e. a negative work-hardening rate at or very near to the yield point. The band in Fig. 7b is extremely fine ($\sim$ 1 μm in width). It must be emphasized that whilst the shear band is recognized by the intensity of the shear, and the etching response indicates a temperature sufficient for phase transformation or modification of the tempered structure, adiabatic shear initiation only requires that the rate of thermal softening exceed the rate of work hardening, i.e. the material is effectively work-softening. Initiation, by the Zener and Holloman [21] hypothesis, does not require a high-temperature excursion.

5. Conclusion

It has been demonstrated that penetrator failure by fracture and adiabatic shear mechanisms can be inter-

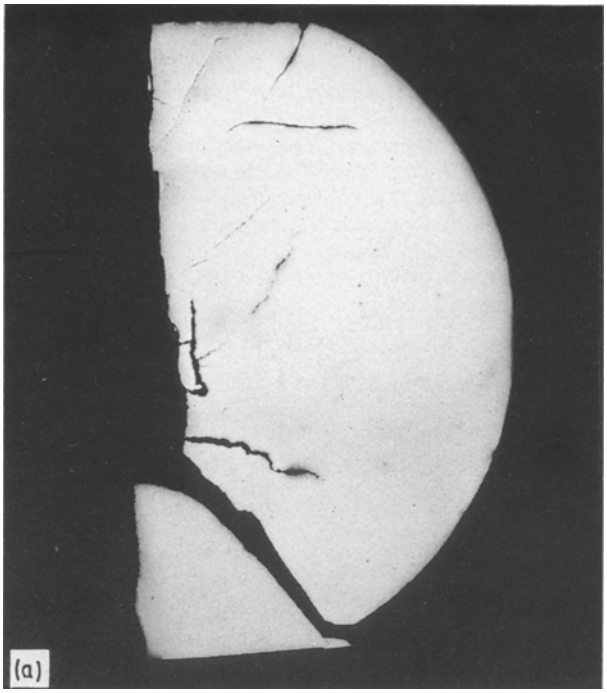

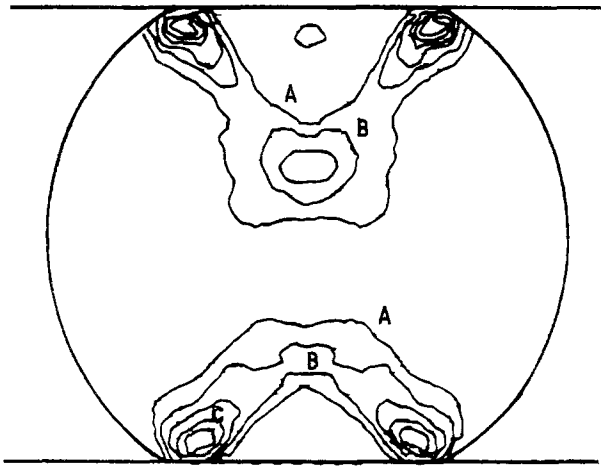

(c)

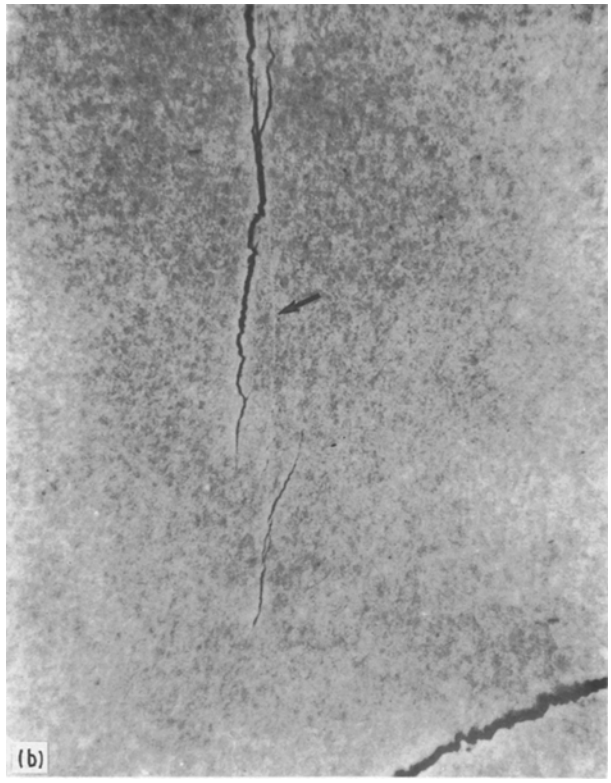

Figure 7 (a) Section through a steel ball compressed quasi-statically between hard platens. The ball has fractured through the centre, a conical region has separated adjacent to one platen and the same failure is incipient at the other. (b) Micrograph of the incipient shear separation of a cone in (a) showing the fine adiabatic shear band (arrow). (c) DYNA 2D simulation showing the contours of maximum shear strain rate for ball compression.

preted in terms of the stress analysis, strain and strain-rate distributions and the material microstructure and properties. Examples from Taylor test impacts as well as penetrator and ball impact studies show a range of failures due to limited ductility, tensile stresses (spalling) and adiabatic shear. It is also demonstrated that some of the observed features can be reproduced in simple quasi-static compression of hard steel balls, which particularly has implications for explanations of the adiabatic shear phenomenon.

References

1. G. I. TAYLOR, *Proc. R. Soc.* **194** (1948) 289.
2. W. JOHNSON, "Impact Strength of Materials" (Arnold, London, 1972).
3. I. M. HUTCHINGS, in "Material Behaviour Under High Stress and Ultrahigh Loading Rates", edited by J. Mescall and V. Weiss, (Plenum, New York, 1982) pp. 161–196.
4. E. H. LEE and S. J. TUPPER, *J. Appl. Mech.* **21** (1954) 63.
5. M. P. WHITE, *ibid.* **51** (1984), 102.
6. J. B. HAWKYARD, *Int. J. Mech. Sci.* **11** (1969) 313.
7. S. E. JONES and P. P. GILLIS, *Int. J. Impact Engng* **4** (1986) 195.
8. S. E. JONES, P. P. GILLIS and J. C. FOSTER Jr, *J. Appl. Phys.* **61** (1987) 499.
9. M. L. WILKINS and M. W. GUINAN, *ibid.* **44** (1973) 1200.
10. R. P. PAPIRNO, J. F. MESCALL and A. M. HANSON, in Proceedings of Army Symposium on Solid Mechanics, 1980: "Designing for Extremes: Environment, Loading and Structural Behaviour", AMMRC MS 80–4, (Watertown, MA, 1980) pp. 367–385.
11. D. A. SHOCKEY, in "Metallurgical Applications of Shock-Wave and High-Strain-Rate Phenomena", edited by L. E. Murr, K. P. Standhammer and M. A. Meyers Dekker, New York, 1986) pp. 633–656.
12. R. L. WOODWARD, *Int. J. Mech. Sci.* **24** (1988) 73.
13. *Idem, Int. J. Impact Engng* **51** (1984) 437.
14. *Idem*, in proceedings of 9th International Symposium on Ballistics, Shrivenham, UK (American Defence Preparedness Association, 1986) pp. 431–437.
15. J. D. YATTEAU, R. F. RECHT and D. L. DICKINSON, *ibid.* Vol. 2, pp. 365–374.
16. M. L. WILKINS, *Int. J. Engng Sci.* **16** (1978) 793.
17. P. N. BROOKS, "Ballistic Impact–The Dependence of the Hydrodynamic Transition Velocity on Projectile Tip Geometry", DREV–R–4001/74 (Defence Research Establishment, Valcartier, 1974).
18. P. N. BROOKS and W. H. ERICKSON, "Ballistic Evaluation of Materials for Armour Penetrators", DREV–R–643/71 (Defence Research Establishment, Valcartier, 1971).
19. J. O. HALLQUIST, "Users Manual for DYNA 2D–An Explicit Two Dimensional Hydrodynamic Finite Element Code with Interactive Rezoning and Graphical Display", UCID-18756, Rev. 3 (Lawrence Livermore National Laboratory, 1988).
20. C. J. FLOCKHART, Y. C. LAM, R. G. O'DONNELL and R. L. WOODWARD, in Proceedings of 3rd International Conference on Constitutive Laws for Engineering Materials:

Theory and Applications, University of Arizona, January 1991, Tuscon, 693–696.
21. C. ZENER and J. H. HOLLOMON, *J. Appl. Phys.* **15** (1944) 22.
22. R. F. RECHT, *J. Appl. Mech.* **31E** (1964) 189.
23. A. J. BEDFORD, A. L. WINGROVE and K. R. L. THOMPSON, *J. Austral. Inst. Met.* **19** (1974) 61.
24. J. M. YELLUP and R. L. WOODWARD, *Res. Mechanica* **1** (1980) 41.
25. H. C. ROGERS, *Ann. Rev. Mater. Sci.* **9** (1979) 283.
26. H. C. ROGERS, in "Material Behavior Under High Stress and Ultrahigh Loading Rates", edited by J. Mescall and V. Weiss, (Plenum, New York, 1983) pp. 101–118.
27. C. J. FLOCKHART, R. L. WOODWARD, Y. C. LAM and R. G. O'DONNELL, *Int. J. Impact Engng* **11** (1991) 93.
28. M. STELLY and R. DORMEVAL, in "Adiabatic Shearing in Metallurgical Applications of Shock-Wave and High-Strain-Rate Phenomena", edited by L. E. Murr, K. P. Staudhammer and M. A. Meyers (Dekker, New York, 1986) pp. 607–632.
29. D. E. GRADY and M. E. KIPP, in "Structural Failure", edited by T. Wierzbicki (Wiley, 1989) pp. 1–40.
30. A. TATE, *J. Mech. Phys. Solids* **15** (1967) 387.
31. T. W. WRIGHT, in "Computational Aspects of Penetration Mechanics", edited by J. Chandra and J. E. Flaherty (Springer, Berlin, 1983), pp. 85–106.
32. R. L. WOODWARD, *Int. J. Mech. Sci.*, **24** (1982) 73.

Received 23 July 1991
and accepted 11 March 1992